Preprints of the 2012 20th Mediterranean Conference on Control & Automation (MED), Barcelona, Spain, July 3-6, 2012

Flatness based Control for Electric and Hybrid Electric Vehicle Drivetrains

Benedikt Alt, Felix Antritter and Ferdinand Svaricek *Member, IEEE*

***Abstract*— Up to now feedforward controllers are seldomly used for the control of automotive vehicle drivetrains. This is partially due to the fact that this popular approach which is based on the inversion of a nominal model may become rather involved. In this paper we illustrate the simplicity and efficiency of flatness based feedforward controller design for the drivetrains of electric and hybrid electric vehicles.**

I. INTRODUCTION

The concept of differential flatness has been developed in the 1990s [1], [2] and it guarantees that a parameterization of all system variables with a so-called flat output exists. In many cases the flat output is a very meaningful variable of the system and in some cases the flat ouput is equivalent to its real output. Then, the design of a corresponding trajectory for a setpoint change boils down to a simple interpolation problem. The trajectory then determines the evolution of the system states and the input by the differential parameterization. Consequently, this parameterization gives a lot of insight into the structure of the control system. Especially, this design procedure yields only trajectories which can indeed be tracked by the system, at least at nominal condition. During the last decade many practical applications have shown that differential flatness has become an efficient approach for the analysis and control of linear and nonlinear systems [4], [5], [6].

In spite of the fact that flatness based feedforward controller design has become a popular methodology in many applications, the usual design approach of feedforward controllers in automotive series-production applications is nevertheless still as follows: A strongly simplified nominal plant model Σ is derived, where

$$\Sigma: \; G(s) = \frac{Y(s)}{U(s)} \tag{1}$$

represents the general transfer function of the plant and $U(s)$, $Y(s)$ denote the Laplace-transforms of the control input $u(t)$ and the output $y(t)$, respectively. Then, the corresponding inverse of Σ is derived. If this inverse exists this approach allows to influence the control input such that the output fulfills a transition between two equilibrium points under nominal conditions. However, for certain plants the inverse $G^{-1}(s)$ may not be realizable or the inverse can provoke unstable system behaviour in case of nonminimum phase systems [1], [2].

For linear systems flatness based feedforward controllers can be very favourably used within a two-degree of freedom structure [7]-[9] as shown in Figure 1.

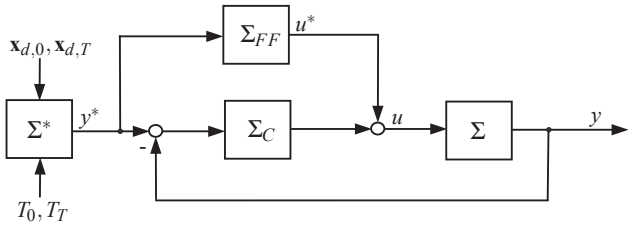

Fig. 1. Two-degree of freedom structure

In this structure the feedback control part can be designed much less aggressive, since it has to deal only with model uncertainties and external disturbances and no longer with the nominal tracking behaviour. This yields a very robust control structure which can also be applied to nonlinear plants. In this contribution the simplicity and efficiency of flatness based feedforward controller design are illustrated by automotive control applications which recently appeared in the field of electric and parallel hybrid electric vehicle (PHEV) drivetrains [10]. Beside the proposed feedforward control design approach for LTI models it will also be shown that nonlinear elements are easy to handle in practical applications. For this purpose a simple drivetrain controller for the electrical machine (EM) speed is augmented such that the influence of a nonlinear torque converter (TC) element can be compensated. The design of the additional feedback controller is done using an optimization based approach similar to [11]-[14] which will not be in the focus of this contribution.

The remainder of this paper is organized as follows: In Section III the drivetrain model of a PHEV with automated manual transmission (AMT) and TC is discussed. In Section IV the principles of flatness based feedforward control design are illustrated. Here, much emphasis is put on the feedforwards for the EM and the nonlinear TC element. Nonlinear simulation results are shown in Section V while Section VI includes a conclusion and an overview of future work.

II. NOTATION

AMT	Automated manual transmission
CAN	Controller area network

B. Alt and F. Svaricek are with the Control Engineering Group, Department of Aeronautical and Space Engineering, University of the German Armed Forces, 85577 Neubiberg, Germany, benedikt.alt@unibw.de

F. Antritter is with the Department of Electrical Engineering, University of the German Armed Forces, 85577 Neubiberg, Germany, felix.antritter@unibw.de

978-1-4673-2529-5/12/$31.00 ©2012 IEEE

EV	Electric vehicle
HEV	Hybrid electric vehicle
ICE	Internal combustion engine
i_t	Transmission ratio [-]
i_d	Transmission ratio final drive [-]
J_2 to J_6	Moment of inertia [kgm^2]
μ	Torque converter torque ratio [-]
ν	Torque converter speed ratio [-]
$\dot{\varphi}_2$ to $\dot{\varphi}_6$	Angular velocity [rad/s]
T_{em}	Electrical machine torque [Nm]
T_{ice}	Combustion torque [Nm]
T_{imp}	Impeller torque of the torque converter [Nm]
T_{rf}	Resistance torque [Nm]
T_{turb}	Turbine torque of the torque converter [Nm]
v_x	Vehicle speed [km/h]

III. MODELING

The control design applications which will be presented in this work appeared recently in the field of PHEV drivetrain control. The structure of the considered drivetrain is depicted in Figure 2.

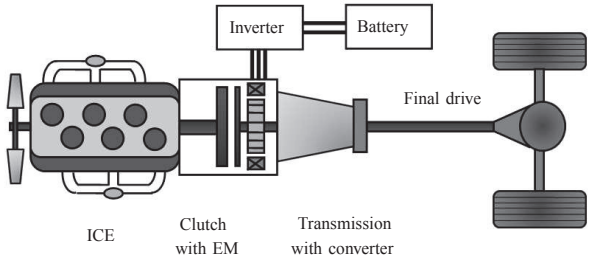

Fig. 2. Drivetrain configuration of PHEV (ICE: Internal combustion engine, EM: Electrical machine)

Here, it can be clearly seen that an internal combustion engine (ICE) and an electrical machine (EM) are able to act on the same drive shaft. In electric operation mode the ICE is decoupled from the rest of the drivetrain by means of a separation clutch migitating the losses of the unfired internal combustion engine and thus leading to an improved overall drivetrain efficiency. Of course, the switching from one operation mode to another requires sophisticated control strategies such as during the synchronization of the ICE and the EM [11]-[13]. However, this contribution focuses on the EM controller which should allow for transitions from one operating point to another in certain driving situations (e.g. during vehicle launch and accelerations). In particular this EM controller has to cope with the fact that the PHEV drivetrain is deduced from an existing conventional vehicle. That means, the drivetrain which has been augmented by a separate HEV module includes still the same automated manual transmission (AMT) and a torque converter (TC) which improves the driving comfort during accelerations. At steady state conditions an additional lock-up clutch is connected in parallel to bypass the torque converter element which would produce too many losses otherwise. For an open lock-up clutch the overall arrangement of the drivetrain is depicted in Figure 3 and the corresponding nonlinear model is derived as follows (see [15]-[17]):

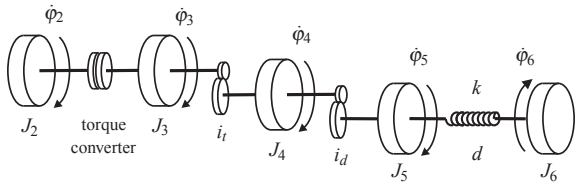

Fig. 3. Parallel hybrid electric vehicle drivetrain (electric operation mode)

$$\begin{bmatrix}\ddot{\varphi}_2\\ \ddot{\varphi}_3\\ \ddot{\varphi}_6\end{bmatrix} = \begin{bmatrix}\frac{1}{J_2}(T_{em}-T_{imp})\\ \frac{1}{J_3'}(T_{turb}-\frac{1}{i}(k(\frac{\varphi_3}{i}-\varphi_6)+d(\frac{\dot{\varphi}_3}{i}-\dot{\varphi}_6)))\\ \frac{1}{J_6}(k(\frac{\varphi_3}{i}-\varphi_6)+d(\frac{\dot{\varphi}_3}{i}-\dot{\varphi}_6)-T_{rf})\end{bmatrix} \quad (2)$$

Here, $T_{imp} = T_{imp}(\dot{\varphi}_2, \dot{\varphi}_3)$, $T_{turb} = T_{turb}(\dot{\varphi}_2, \dot{\varphi}_3)$ and the variables $\dot{\varphi}_2$, $\dot{\varphi}_3$, $\dot{\varphi}_6$ denote the angular velocities of the EM, the turbine side of the torque converter and the wheels, respectively. The inertias J_3 to J_5 are lumped into

$$J_3' = J_3 + \frac{J_4}{i_t^2} + \frac{J_5}{i^2} \quad (3)$$

and the variables i_t, i_d and $i = i_t i_d$ denote the gear transmission ratios of the automatic transmission, the final drive and the overall drivetrain, respectively. The variable T_{rf} denotes the torque due to the vehicle resistance forces such as road friction, air drag and climbing resistance.

For the calculation of the impeller torque T_{imp} and the turbine torque T_{turb} a well-known automotive modeling approach for torque converters is introduced [18]. For this purpose the nonlinear characteristic maps $T_{imp}^* = T_{imp}^*(\nu)$ and $T_{turb}^* = T_{turb}^*(\nu)$ have to be determined at a fixed impeller speed $\dot{\varphi}_2^*$. Here, the variables

$$\nu^* = \frac{\dot{\varphi}_3}{\dot{\varphi}_2^*}, \quad \nu = \frac{\dot{\varphi}_3}{\dot{\varphi}_2}, \quad (4)$$

denote the ratio of the angular velocity $\dot{\varphi}_3$ at the turbine side and $\dot{\varphi}_2^*$, $\dot{\varphi}_2$, respectively. If $\nu = \text{const.}$ and the ratio between $\dot{\varphi}_2^2$ and T_{imp} can be considered as fixed for each impeller angular velocity $\dot{\varphi}_2$, the impeller torque T_{imp} and the turbine torque T_{turb} can be calculated with

$$T_{imp} = T_{imp}^*(\nu)\left(\frac{\dot{\varphi}_2}{\dot{\varphi}_2^*}\right)^2 = \frac{1}{K^2(\nu)}\dot{\varphi}_2^2, \quad (5)$$

$$T_{turb} = \mu^*(\nu)\, T_{imp}^*(\nu)\left(\frac{\dot{\varphi}_2}{\dot{\varphi}_2^*}\right)^2, \quad (6)$$

where

$$K(\nu) = \frac{\dot{\varphi}_2^*}{\sqrt{T_{imp}^*(\nu)}} \text{ and } \mu = \mu^* = \frac{T_{turb}^*}{T_{imp}^*} \quad (7)$$

represents the TC ratio. The corresponding characteristic maps of $T_{imp}^*(\nu)$ and $\mu^*(\nu)$ are depicted in Figure 4.

For the flatness-based feedforward controller design for the overall PHEV drivetrain the known TC model from [18] has to be modified in order to obtain mathematical expressions which are suitable for system inversion.

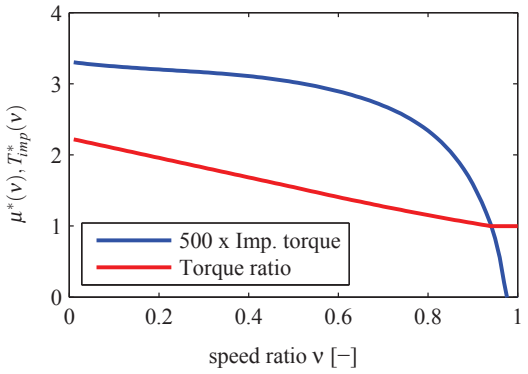

Fig. 4. Torque converter characteristic maps, $T^*_{imp}(\nu)$ (blue), $\mu^*(\nu)$ (red)

For this purpose the separated rotational dynamics of the TC can be rewritten as

$$\begin{bmatrix}\ddot{\varphi}_2\\ \ddot{\varphi}_3\end{bmatrix} = \begin{bmatrix}\frac{1}{J_2}(T_{em} - F_1(\nu)\dot{\varphi}_3^2)\\ \frac{1}{J_3}F_2(\nu)\dot{\varphi}_3^2\end{bmatrix} \tag{8}$$

where $F_1(\nu) = \frac{1}{K^2(\nu)\nu^2}$ and $F_2(\nu) = \frac{\mu(\nu)}{K^2(\nu)\nu^2}$.

Here, it can be shown that $\mu'(\nu) = \mu_0 - \frac{d\mu}{d\nu}\nu$ provides a good approximation for $\mu(\nu)$. From Figure 5 it can be seen that

$$F_1' \approx \frac{\gamma}{\nu^2} \text{ and } F_2' \approx \frac{\gamma\mu'(\nu)}{\nu^2} \tag{9}$$

yield also good approximations for $F_1(\nu)$ and $F_2(\nu)$ in (8). Additionally, they fulfill the aforementioned requirement on system inversion as well.

Finally, the EM is modeled as pure torque source and its closed-loop torque modulation can be approximated with a first order lag while the time-varying CAN Bus communication delay is upper bounded by a conservative limitation δ_{em}:

$$\dot{T}_{em} = \frac{1}{\tau_{em}}\left(T_{em,ref}(t-\delta_{em}) - T_{em}\right) . \tag{10}$$

IV. CONTROL DESIGN

A. Mathematical preliminaries

First, some preliminaries on differential flatness are briefly revisited. For this purpose a nonlinear single-input system

$$\dot{\mathbf{x}}(t) = \mathbf{f}(\mathbf{x}(t), u(t)) , \tag{11}$$

with $\mathbf{x} \in \mathscr{X} \subset \mathbb{R}^n$, $u \in \mathscr{U} \subset \mathbb{R}$ will be considered. The system in (11) is called flat, if there exists a flat output

$$y_f = h_f(\mathbf{x}) , \tag{12}$$

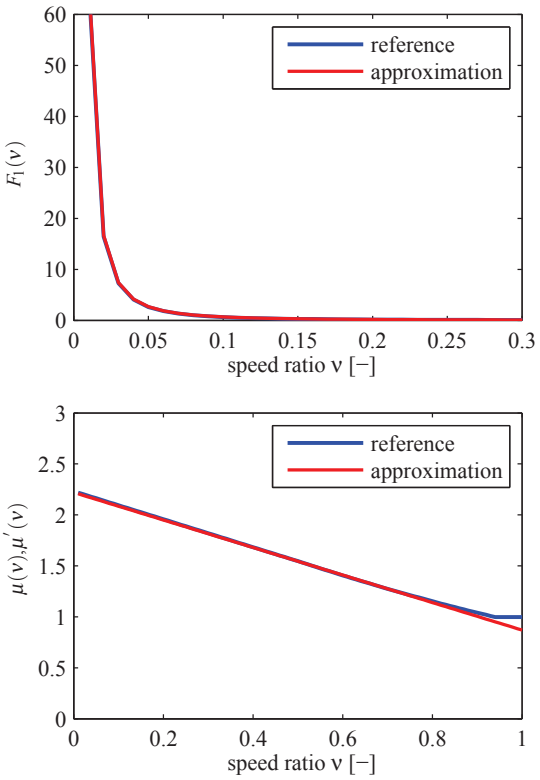

Fig. 5. Comparison of $F_1(\nu)$ and $F_1'(\nu)$ (up) and $\mu(\nu)$ and $\mu'(\nu)$ (bottom)

which allows a differential parameterization of the states and the input

$$\mathbf{x} = \psi_x(y_f, \dot{y}_f, \ldots, y_f^{(n-1)}) , \tag{13}$$

$$u = \psi_u(y_f, \dot{y}_f, \ldots, y_f^{(n)}) . \tag{14}$$

Thus, to every sufficiently smooth desired trajectory $y_{f,d} : I \subset \mathbb{R} \to \mathbb{R}$ there exists a corresponding state trajectory

$$\mathbf{x}_d(t) = \psi_x(y_{f,d}(t), \dot{y}_{f,d}(t), \ldots, y_{f,d}^{(n-1)}(t)), \tag{15}$$

with $t \in I = [t_0, t_f]$, which is indeed a solution of (11). If the initial conditions satisfy the user requirements on

$$\mathbf{x}(t_0) = \psi_x(y_{f,d}(t_0), \dot{y}_{f,d}(t_0), \ldots, y_{f,d}^{(n-1)}(t_0)) \tag{16}$$

the corresponding feedforward controller which achieves the desired trajectory is given with

$$u_d(t) = \psi_u(y_{f,d}(t), \dot{y}_{f,d}(t), \ldots, y_{f,d}^{(n)}(t)) \tag{17}$$

for $t \in I$.

In the following steps we consider the class of linear time invariant (LTI) systems. These systems are flat if and only if they are controllable [1], [2]. Then, any controllable linear system

$$\begin{aligned}\dot{\mathbf{x}}(t) &= \mathbf{A}\mathbf{x}(t) + \mathbf{b}u(t) ,\\ y(t) &= \mathbf{c}^T\mathbf{x}(t) ,\end{aligned} \tag{18}$$

with $\mathbf{x} = [x_1, \ldots, x_n]^T \in \mathbb{R}^n$, $u \in \mathbb{R}$ can be transformed into its controllability form (see [19]) with a suitable state transformation $\mathbf{z} = \mathbf{T}\mathbf{x}$:

$$\dot{\mathbf{z}} = \begin{bmatrix} 0 & 1 & \cdots & 0 \\ \vdots & & \ddots & \vdots \\ 0 & & & 1 \\ -a_0 & \cdots & \cdots & -a_{n-1} \end{bmatrix} \mathbf{z} + \begin{bmatrix} 0 \\ \vdots \\ 0 \\ 1 \end{bmatrix} u \ , \qquad (19)$$

where $\mathbf{z} = [z_1, \ldots, z_n]^T \in \mathbb{R}^n$. In view of (19) it is obvious that z_1 is a flat output, since clearly

$$[z_1, z_2, \ldots, z_n]^T = [y_f, \dot{y}_f, \ldots, y_f^{(n-1)}]^T \ . \qquad (20)$$

Consequently, the parametrization of u is given with

$$u_d = a_0 y_f + \cdots + a_{n-1} y_f^{(n-1)} \ . \qquad (21)$$

For more information and a detailed characterization of flat outputs for linear systems the reader is referred to [1], [2]. In the remainder of this Section we will present three recent applications within the field of EV and HEV drivetrain control. Note, that the torque control design example in Section IV-B represents also a baseline for the following speed controllers in Sections IV-C and IV-D.

B. Torque controller

In electric driving mode the subordinated EM feedback controller calculates the voltages and the currents inside the EM such that the desired torque T_{em}[1] tracks a given reference value $T_{em,ref}$ which is computed by supervisory algorithms (e.g. in Sections IV-C and IV-D).

From the dynamics of the closed-loop torque modulation in eq. (10) it can be clearly seen that the underlying system is not able to realize step-wise inputs in T_{em}. However, the trajectory of the EM torque T_{em} can be directly influenced if the dynamic system behaviour is incorporated within the calculation of the reference value $T_{em,ref}$. Thus, this novel feedforward controller calculates this input $T_{em,ref}$ to the closed-loop system such that its output T_{em} realizes the desired trajectory $T_{em,d}$ at nominal condition. For this purpose the model of the closed-loop system in (10) is split up into a first order lag and a time delay as shown in Figure 6.

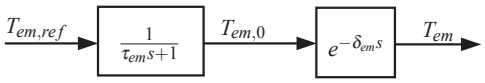

$$\tau_{em}\dot{T}_{em,0} + T_{em,0} = T_{em,ref} \quad T_{em} = T_{em,0}(t - \delta_{em})$$

Fig. 6. Block diagram for EM torque controller design

Similar to the design procedure in (18)-(21) the torque $T_{em,0}$ can be also considered as flat output. Consequently, the reference value $T_{em,ref}$ for the subordinated closed-loop system is calculated from the resulting feedforward controller

$$T_{em,ref} = \tau_{em}\dot{T}_{em,0,d} + T_{em,0,d} \ . \qquad (22)$$

[1]It is assumed that there exist appropriate algorithms to estimate T_{em} from the available measurements.

To alleviate the effects which are related to the delay time δ_{em} the desired EM torque $T_{em,0,d}$ is calculated from the shifted torque trajectory $T_{em,d}$ which serves as input signal to the feedforward controller for the EM torque:

$$T_{em,0,d} = T_{em,d}(t + \delta_{em}) \ . \qquad (23)$$

C. Speed controller

Beside the electric torque T_{em} the angular velocity $\dot{\varphi}_2$ of the EM represents also an interesting control variable for a high-level controller in certain driving situations (e.g. vehicle launch of an electric vehicle). Since the plant of the underlying closed-loop torque modulation is augmented by its corresponding rotational dynamics

$$G^*_{rot}(s) = \frac{\dot{\varphi}_2(s)}{T_{em}(s)} = \frac{1}{J_2 s} \ , \qquad (24)$$

the following speed control law can be interpreted as an extension of the torque controller in Section IV-B. For this purpose the block diagram of the overall plant is depicted in Figure 7.

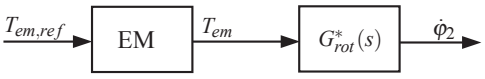

Fig. 7. Block diagram for EM speed controller design

Now, the reference trajectory for $T_{em,d}$ is updated at each time step t_k by means of a corresponding reference trajectory for $\dot{\varphi}_{2,d}$. If any supervisory control algorithm requests a step-wise change in $\dot{\varphi}_2$ an additional realtime trajectory generator computes a smooth reference trajectory, i.e.

$$\dot{\varphi}_{2,d}(t_k) = \gamma_3 t_k^3 + \gamma_2 t_k^2 + \gamma_1 t_k + \gamma_0 \ , \qquad (25)$$

with γ_0, γ_1, γ_2, $\gamma_3 \in \mathbb{R}$ and

$$\dot{\varphi}_{2,d}(t_k) = \dot{\varphi}_{2,d}(t_{k-1})\,\frac{\text{rad}}{\text{s}}, \quad \dot{\varphi}_d(t_k + T_t) = \dot{\varphi}_{2,d,end}\,\frac{\text{rad}}{\text{s}} \qquad (26)$$

$$\ddot{\varphi}_{2,d}(t_k) = \ddot{\varphi}_{2,d}(t_{k-1})\,\frac{\text{rad}}{\text{s}^2}, \quad \ddot{\varphi}_{2,d}(t_k + T_t) = \ddot{\varphi}_{2,d,end}\,\frac{\text{rad}}{\text{s}^2} \qquad (27)$$

such that the condition $\dot{\varphi}_2 = \dot{\varphi}_{2,end}$ is satisfied within a given transition time $T_t = n \cdot t_k$ where $n > 1$. As stated above it has to be guaranteed that the reference signal $\dot{\varphi}_{2,d}$ is sufficiently smooth and additionally all required derivatives must exist. Then, the desired trajectory on the EM torque is given with

$$T_{em,d}(t_k) = J_2 \ddot{\varphi}_{2,d}(t_k) \ . \qquad (28)$$

For a representative launch maneuver of an electric vehicle where $\dot{\varphi}_{2,d}(t_k) = \ddot{\varphi}_{2,d}(t_k) = 0\frac{\text{rad}}{\text{s}}$ and $\ddot{\varphi}_{2,d}(t_k + T_t) = 0\frac{\text{rad}}{\text{s}^2}$ the reference trajectory parameters result in

$$\gamma_0 = 0, \gamma_1 = 0, \gamma_2 = \frac{3\dot{\varphi}_{2,d,end}}{T_t^2} \text{ and } \gamma_3 = -\frac{2\dot{\varphi}_{2,d,end}}{T_t^3} \ . \qquad (29)$$

Then, the desired trajectory on the EM torque is given with

$$T_{em,d}(t_k) = 6J_2\left(\frac{\dot{\varphi}_{2,d,end} t_k}{T_t^2} - \frac{\dot{\varphi}_{2,d,end} t_k^2}{T_t^3}\right) \ . \qquad (30)$$

D. Speed controller with torque converter compensation

In a further extension the EM speed controller will be tasked to control directly the wheel angular velocity $\dot{\varphi}_6$ instead of $\dot{\varphi}_2$. This feedforward control algorithm will allow for almost jerkless vehicle launch and accelerations at nominal condition. However, in the underlying PHEV vehicle configuration $\dot{\varphi}_6$ is not equal to $\dot{\varphi}_2$ neither at steady state nor in transient conditions. Thus, simplified models for the automated manual transmission (AMT) and the torque converter have to be incorporated within the feedforward control design. To keep the feedforward design task as simple as possible the elastic spring element of the side axle will however not be considered within the design. Instead, the corresponding effects will be alleviated by means of the feedback controller within the two-degree of freedom structure. Since the design of the feedforward controller is closely related to Section IV-C the following explanations will focus on the major differences between both algorithms. Now, the reference trajectory for $\dot{\varphi}_{6,d}$ represents the starting point of the design and it will be calculated similar to (25)-(28) from a given step-wise change for $\dot{\varphi}_6$. The resulting reference trajectory $\dot{\varphi}_{6,d}$ will be shifted to the angular velocity $\dot{\varphi}_{3,d}$ at the turbine side of the TC by means of the AMT and final drive overall conversion ratio $i = i_t i_d$ using $\dot{\varphi}_{3,d} = \frac{1}{i}\dot{\varphi}_{6,d}$. In the subsequent steps the reference value ν_d for the TC speed ratio can be computed from the mathematical approximation of the TC model in Section III and $\dot{\varphi}_{3,d}$ as well as its time derivative $\ddot{\varphi}_{3,d}$:

$$\nu_d = F_2^{'(-1)}\left(J_3'\frac{\ddot{\varphi}_{3,d}}{\dot{\varphi}_{3,d}^2}\right) . \tag{31}$$

Then, since $\dot{\varphi}_{3,d}$ and ν_d are symbolically known it is easy to compute the reference value

$$\dot{\varphi}_{2,d} = \frac{\dot{\varphi}_{3,d}}{\nu_d} \tag{32}$$

for the EM angular velocity at the impeller side of the TC (see (4)). Additionally, we can also compute the corresponding angular acceleration

$$\ddot{\varphi}_{2,d} = \frac{\ddot{\varphi}_{3,d}\nu_d - \dot{\varphi}_{3,d}\dot{\nu}_d}{\nu_d^2} . \tag{33}$$

Finally, the corresponding reference trajectory $T_{em,d}$ for the EM torque within a PHEV drivetrain is given (see (8), (9)) with

$$T_{em,d} = J_2\ddot{\varphi}_{2,d} + F_1'\dot{\varphi}_{3,d}^2 . \tag{34}$$

E. Feedback controller

The feedforward controls from Sections IV-B, IV-C and IV-D are based on simplified drivetrain models which hold true for the nominal condition. No external disturbances such as overall resistance force, elastic springs or model uncertainties are taken into account. Thus, it can not be expected, that a pure feedforward control framework guarantees a perfect tracking of the reference signal $\dot{\varphi}_{2,d}$ or $\dot{\varphi}_{6,d}$ in the end. For this purpose an additional tracking controller is introduced either on $\dot{\varphi}_2$ or even on $\dot{\varphi}_6$ within the two-degree of freedom structure which stabilizes the corresponding trajectory. Since the corresponding design steps are well known from literature [20] the description will be omitted here due to space restrictions.

V. NONLINEAR SIMULATION

This section illustrates the efficiency of the proposed feedforward control design approach. For this purpose a detailed simulation study has been carried out with a nonlinear simulation model which is similar to that in [17]. This simulation model includes in particular nonlinear and elastic spring elements within the side axles and the resistance forces. Due to space restrictions we show only representative results for the PHEV drivetrain without and with torque converter element. Here, we show a comparison of two feedforward controllers during a vehicle launch maneuver where the vehicle will be accelerated up to $\dot{\varphi}_{6,d,end} = 5\frac{\text{rad}}{\text{s}}$ ($v_{x,end} \approx 5.6$ km/h). The corresponding simulation results are depicted in Figure 8 and they include three case studies. In *case 1* we design the controller similar to Section IV-C where we consider only the rigid drivetrain without TC element (here, the control design is adjusted to the wheel angular velocity $\dot{\varphi}_6$). In *case 2* we use the same controller from *case 1* but consider a drivetrain with TC element. In this case we see directly that the simple feedforward controller from *case 1* leads to large deviations from the desired trajectory $\dot{\varphi}_{6,d}$. Thus, the additional feedback controller would have to alleviate these effects which would lead to additional calibration efforts. Finally in *case 3*, we apply the extended speed controller from Section IV-D which allows to compensate impressively for the effects which are induced by the nonlinear TC element. Thus, the additional feedback controller can be tuned much less aggressive.

VI. CONCLUSION AND FUTURE WORK

This paper focuses on the two-degree of freedom structure which represents an interesting design approach for many automotive applications which appeared recently in the field of EVs and PHEVs. In particular, we concentrate on the feedforward control design which relies on a suitable LTI model of the plant and a flatness based design approach. Here, we present three application examples for EM torque and EM speed control. For the speed control we consider also a PHEV drivetrain where the influence of a TC has to be compensated.

Future work will concentrate on a rigorous Lyapunov analysis [21], [22], [23] for the nonlinear closed-loop system and a practical implementation on a research vehicle. Here, the realtime trajectory generation within a series-production software standard and the switchings from one control mode to another represent interesting research fields.

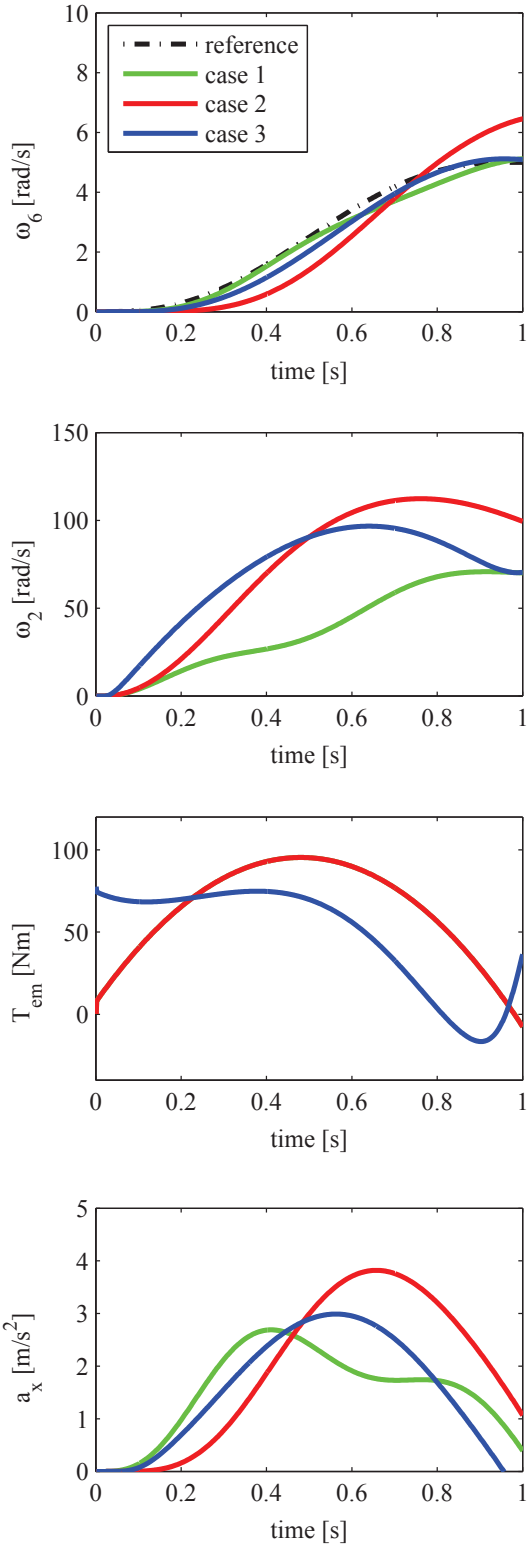

Fig. 8. Nonlinear simulation results, EM angular velocity $\omega_6 = \dot{\varphi}_6$ (first), wheel angular velocity $\omega_2 = \dot{\varphi}_2$ (second), EM torque T_{em} (third), longitudinal acceleration a_x (fourth)

VII. ACKNOWLEDGMENT

This work has been supported by IAV GmbH Gifhorn in Germany. The authors express their gratitude to Matthias Schultalbers and his colleagues for their support.

REFERENCES

[1] M. Fliess, J. Lévine, P. Martin, and P. Rouchon. Flatness and defect of nonlinear systems: introductory theory and examples. *Int. J. Control*, 61(6), 1995, pp. 1327 – 1361.

[2] M. Fliess, J. Lévine, P. Martin, and P. Rouchon. A Lie-Bäcklund approach to equivalence and flatness of nonlinear systems. *IEEE Trans. Automat. Control*, 44 (5), 1999, pp. 922 – 937.

[3] J. Lévine. Are there new industrial perspectives in the control of mechanical systems? In P. Frank, editor, *Advances in Control, Highlights of ECC'99*, Springer, London, 1999.

[4] J. Lévine and B. Rémond. Flatness based control of an automatic clutch. *In Proceedings of the MTNS-2000*, Perpignan, France, 2000.

[5] P. Martin, R.M. Murray and P. Rouchon. Flat systems. In G. Bastin and M. Gevers, editors, *Plenary Lectures and Minicourses, Proc. ECC 97, Brussels*, 1997, pp. 211 – 264.

[6] B. Kiss, J. Lévine and P. Mullhaupt: Control of a reduced size model of US Navy Crane using only motor position sensors. In A. Isidori, F. Lamnabhi-Lagarrgigue, W. Respondek: *Nonlinear Control in the Year 2000*, Lecture Notes in Control and Information Sciences 259.

[7] I.M. Horowitz, *Synthesis of Feedback Systems*, Academic Press, New York, USA, 1963

[8] N. Zimmert and O. Sawodny. Active damping control for bending oscillations of a forklift mast using flatness based techniques, *Proceedings of the 2010 American Control Conference*, Baltimore, MD, USA, 2010.

[9] B. Alt, F. Antritter, F. Svaricek, F. Wobbe, T. Boehme and M. Schultalbers. Two degree of freedom structure for reduction of driveline oscillations, *Proceedings of the AUTOREG 2011*, Baden Baden, Germany, 2011.

[10] J. Boehle and B. Stiebels, Der neue Touareg Hybrid, *ATZ extra - Der VW Touareg*, vol. 2, 2010.

[11] J.P. Blath. A multivariable speed controller for a hybrid electric vehicle, *Proceedings of the 4th ASIM Workshop*,Wismar, Germany, 2008.

[12] R. Gasper, R. Beck, P. Drews and D. Abel. Feedforward control of a parallel hybrid launch clutch, *Proceedings of the European Control Conference*, Budapest, Hungary, 2009.

[13] B. Alt, F. Antritter, F. Svaricek, J.P. Blath and M. Schultalbers. Improved performance for the synchronization of the angular velocity in hybrid electric vehicles using a feedforward strategy, *Proceedings of the IFAC Symposium Advances in Automotive Control*, Munich, Germany, 2010.

[14] B. Alt, F. Antritter, F. Svaricek and M. Schultalbers. A model based control design approach for powertrain control of a parallel hybrid electric vehicle (in german), *AT-Automatisierungstechnik*, 58(10), 2010, pp. 568 – 579.

[15] U. Kiencke and L. Nielsen. *Automotive control systems, 2nd edition*, Springer Verlag, Berlin, Heidelberg, New York, 2000.

[16] L. Guzzella and C.H. Onder. *Introduction to modeling and control of internal combustion engine systems*, Springer Verlag, Berlin, Heidelberg, New York, 2004.

[17] B. Alt. *Modellbasierte Regelung ausgewaehlter Komponenten im Antriebsstrang eines Kraftfahrzeugs mit Ottomotor*, PhD Thesis, VDI, Verlag, Duesseldorf, Germany, 2010.

[18] H. Naunheimer, B. Bertsche and G. Lechner. *Fahrzeuggetriebe*, Springer-Verlag, Berlin, Heidelberg, Germany, 2007.

[19] T. Kailath. *Linear Systems*, Prentice-Hall, Englewood-Cliffs, USA, 1980.

[20] A. Visioli. *Practical PID Control*, Springer Verlag, Berlin, Heidelberg, New York, 2006.

[21] A. Isidori. *Nonlinear control systems II*, Springer Verlag, Berlin, Heidelberg, New York, 1999.

[22] H.K. Khalil, Nonlinear Systems, Prentice Hall, Upper Saddle River, 2002

[23] F. Antritter, *Tracking Controller Design for nonlinear dynamics using differential parameterizations*, PhD Thesis, Shaker-Verlag, Aachen, Germany, 2007